

Spectra and structure functions in nonhelical hydromagnetic turbulence

Nils Erland L. Haugen*

Department of Physics, The Norwegian University of Science and Technology, Høyskoleringen 5, N-7034 Trondheim, Norway

Axel Brandenburg†

NORDITA, Blegdamsvej 17, DK-2100 Copenhagen Ø, Denmark

Wolfgang Dobler‡

Kiepenheuer-Institut für Sonnenphysik, Schöneckstraße 6, D-79104 Freiburg, Germany

(Dated: February 7, 2020, Revision: 1.39)

Nonhelical hydromagnetic turbulence without imposed magnetic field is considered. The magnetic field is entirely due to dynamo action. The structure function exponents scale approximately like in nonmagnetic turbulence and follow the She-Leveque scaling for predominantly one-dimensional (tube-like) dissipative structures. Throughout the inertial range the spectral magnetic energy exceeds the kinetic energy by a factor of 2 to 3, and both spectra are approximately parallel. At first glance, the total energy spectrum seems to be close to $k^{-3/2}$, but there is a strong bottleneck effect and it is suggested that the asymptotic spectrum is $k^{-5/3}$. This is supported by the value of the second order structure function exponent that is found to be $\zeta_2 = 0.70$, suggesting a $k^{-1.70}$ spectrum.

Many astrophysical environments are in a turbulent state. Examples include the solar convection zone, the solar wind, the gaseous discs around young stars or compact objects, the interstellar medium and clusters of galaxies. In most of these cases the gas is fully ionized and part of the kinetic energy of the turbulence is converted into magnetic energy via dynamo action. This gives rise to the question how turbulence is affected by dynamo processes and whether Kolmogorov's description of isotropic turbulence is still a reasonable approximation. In the present case we are particularly interested in the case without helicity. In the presence of helicity there is an inverse cascade of magnetic helicity producing large scale fields [1], which has been studied in detail elsewhere [2, 3, 4]. Our current understanding of nonhelical hydromagnetic turbulence is still uncertain partly because so many different results have been obtained in a range of different circumstances: with or without imposed fields, for decaying or forced turbulence, compressible or incompressible fluids, at modest or large resolution (and Reynolds number), large or small magnetic Prandtl numbers, and with or without hyperviscosity and hyper-resistivity.

In this Letter we are interested in the form of the magnetic and kinetic energy spectra in the inertial range where the turbulence is driven at large scales and the magnetic field is self-generated. This problem is a generalization of Kolmogorov turbulence to a fluid that is electrically conducting. If the conductivity is large enough, which is the case in many astrophysical settings, a magnetic field will inevitably grow and then saturate at a

dynamically important level.

An important question is whether there is equipartition at small scales, or whether the magnetic energy is even dominated by contributions from small scales [4, 5]. A difficulty in assessing the small scale contributions has been the lack of a sufficiently long inertial range. In some cases the use of hyper-resistivity has led to the concern that it may cause an artificially strong 'bottleneck effect' with a shallower k^{-1} spectrum just before the dissipative subrange [6]. Yet another problem is the possibility of a physical bottleneck effect [7] that will be more extreme in three-dimensional spectra than in the one-dimensional spectra accessible from turbulence experiments [6, 8].

Here we consider subsonic turbulence in an isothermal electrically conducting gas with constant sound speed c_s in a periodic box of size $2\pi \times 2\pi \times 2\pi$. The governing equations are

$$\frac{D\mathbf{u}}{Dt} = -c_s^2 \nabla \ln \rho + \frac{\mathbf{J} \times \mathbf{B}}{\rho} + \mathbf{F}_{\text{visc}} + \mathbf{f}, \quad (1)$$

where $D/Dt = \partial/\partial t + \mathbf{u} \cdot \nabla$ is the advective derivative, $\mathbf{J} = \nabla \times \mathbf{B}/\mu_0$ the current density, \mathbf{B} the magnetic field, μ_0 the vacuum permeability,

$$\mathbf{F}_{\text{visc}} = \nu (\nabla^2 \mathbf{u} + \frac{1}{3} \nabla \nabla \cdot \mathbf{u} + 2\mathbf{S} \cdot \nabla \ln \rho) \quad (2)$$

is the viscous force where $\nu = \text{const}$ is the kinematic viscosity, $\mathbf{S}_{ij} = \frac{1}{2}(u_{i,j} + u_{j,i}) - \frac{1}{3}\delta_{ij}u_{k,k}$ is the traceless rate of strain tensor, and \mathbf{f} is a random forcing function (see below). The continuity equation is written in terms of the logarithmic density,

$$\frac{D \ln \rho}{Dt} = -\nabla \cdot \mathbf{u}, \quad (3)$$

and the induction equation is solved in terms of the magnetic vector potential \mathbf{A} , where $\mathbf{B} = \nabla \times \mathbf{A}$, and

$$\frac{\partial \mathbf{A}}{\partial t} = \mathbf{u} \times \mathbf{B} + \eta \nabla^2 \mathbf{A}, \quad (4)$$

*Electronic address: nils.haugen@phys.ntnu.no

†Electronic address: brandenb@nordita.dk

‡Electronic address: Wolfgang.Dobler@kis.uni-freiburg.de

where $\eta = \text{const}$ is the magnetic diffusivity; we choose $\eta = \nu$, i.e. our magnetic Prandtl number is unity. We adopt a forcing function \mathbf{f} of the form

$$\mathbf{f}(\mathbf{x}, t) = \text{Re}\{N \mathbf{f}_{\mathbf{k}(t)} \exp[i\mathbf{k}(t) \cdot \mathbf{x} + i\phi(t)]\}, \quad (5)$$

where $\mathbf{x} = (x, y, z)$ is the position vector, and $-\pi < \phi(t) < \pi$ is a (δ -correlated) random phase. The normalization factor is $N = f_0 c_s (kc_s/\delta t)^{1/2}$, with f_0 a nondimensional forcing amplitude, $k = |\mathbf{k}|$, and δt the length of the timestep; we chose $f_0 = 0.02$ so that the maximum Mach number stays below about 0.5 (the rms Mach number is close to 0.2 in all runs.) The vector amplitude \mathbf{f}_k describes nonhelical transversal waves with $|\mathbf{f}_k|^2 = 1$ and

$$\mathbf{f}_k = (\mathbf{k} \times \mathbf{e}) / \sqrt{\mathbf{k}^2 - (\mathbf{k} \cdot \mathbf{e})^2}, \quad (6)$$

where \mathbf{e} is an arbitrary unit vector. At each timestep we select randomly one of 20 possible wavevectors in the range $1 \leq |\mathbf{k}| < 2$ around the forcing wavenumber, $k_f = 1.5$.

The equations are solved using the same method as in Ref. [3], but here we employ a new cache and memory efficient code [9] using MPI (Message Passing Interface) library calls for communication between processors. This allows us to run quite easily at a resolution of 512^3 meshpoints.

In Fig. 1 we plot magnetic, kinetic, and total energy spectra, $E_M(k)$, $E_K(k)$, and $E_T = E_M + E_K$, respectively, for our largest resolution run with 1024^3 meshpoints. The magnetic energy displays a nearly flat spectrum in the range $1 \leq k \leq 5$ and begins to show an inertial range in $8 \leq k \leq 25$, followed by a dissipative subrange over one decade. In the inertial range $E_M(k)/E_K(k)$ is about 2.5.

The energy ratio in the inertial range is similar to the ratio of the dissipation rates of magnetic and kinetic energies which is about 2.3; see Fig. 2, which shows that magnetic and kinetic energy dissipation rates approach 70% and 30%, respectively, of the total dissipation rate. The convergence of relative dissipation rates is compatible with Kolmogorov's concept of a constant scale independent energy flux across the spectrum, which seems to apply here even separately for velocity and magnetic fields. We emphasize that the inertial range is not representative of the total energy which, in turn, is dominated by small wavenumbers. The ratio of total magnetic to kinetic energies is only 0.4 and seems again to be asymptotically independent of Reynolds number (Fig. 2).

By comparing runs at different resolution one can clearly see that in the range $3 \leq k \leq 20$ the total energy spectrum is shallower than $k^{-5/3}$ (Fig. 3). This could perhaps be due to the bottleneck effect that is known to exist also in wind tunnel turbulence, where it has been described by a weak k^{-1} contribution [10]. In the present context such a contribution could be much stronger. There are at least three possible explanations for this difference. First, the bottleneck effect is much stronger in shell integrated three-dimensional spectra compared to just longitudinal or transversal one-dimensional spectra available in wind tunnel turbulence [8]. Second,

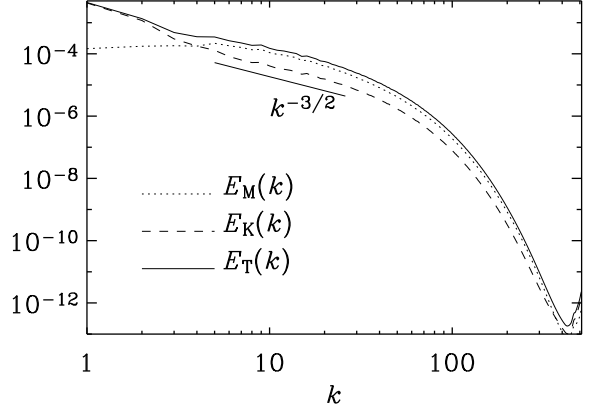


FIG. 1: Magnetic, kinetic and total energy spectra. 1024^3 meshpoints. The Reynolds number is $u_{\text{rms}}/(\nu k_f) \approx 960$.

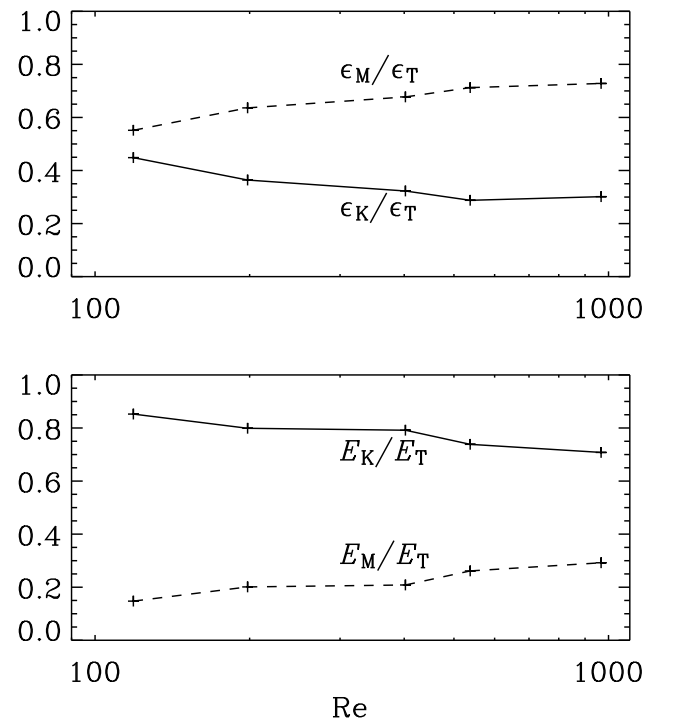


FIG. 2: Approximate convergence of relative magnetic and kinetic energy dissipation rates (upper panel) and the relative energies (lower panel) as a function of Reynolds number.

the bottleneck effect may simply be stronger for hydro-magnetic turbulence due to the dynamo effect that is expected to produce magnetic energy preferentially at $k = k_f R_c^{1/2} \approx 8$, where $R_c \approx 25$ is the critical magnetic Reynolds number for dynamo action [11]. Third, numerical effects such as hyperdiffusion or other effects causing departures from the physical ∇^2 diffusion operator could cause an artificial bottleneck effect [6, 12], which may also explain the extended k^{-1} range in compressible nonmagnetic simulations using the piecewise parabolic method

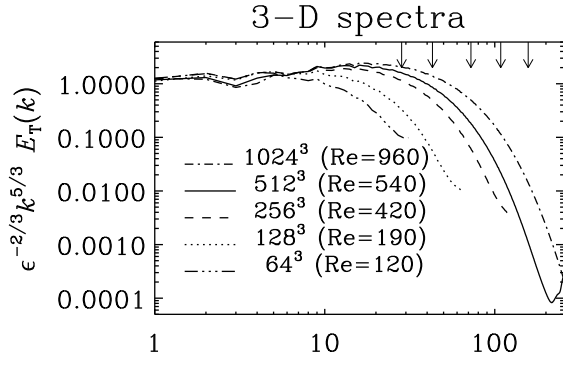


FIG. 3: Total energy spectra compensated by $\epsilon^{-2/3} k^{5/3}$, where ϵ is the rate of total energy dissipation. Spectra for different resolution are compared. The dissipation cutoff wavenumber, $k_d = (\epsilon/\nu^3)^{1/4}$, is indicated by short arrows at the top of the plot. The Reynolds number, $Re = u_{\text{rms}}/(\nu k_f)$, is given in the legend. The lower panel shows the same for longitudinal spectra.

[13].

We believe that numerical effects do not cause such artifacts in our simulations, because we use the physical ∇^2 diffusion operator and our discretization is accurate to sixth order in space and third order in time. We have compared two runs with identical values of ν and η , one with 256^3 meshpoints and the other one with 512^3 , and found the same spectra [14]. We have also compared with runs using double precision and found the spectra to be the same.

We do not know whether the bottleneck effect is really stronger in hydromagnetic turbulence, but it is certainly weaker in one-dimensional spectra [8]. It is therefore still possible that at larger Reynolds numbers the true inertial range spectrum will have a $k^{-5/3}$ behavior both for kinetic and magnetic energies [15].

Alternatively, a $k^{-3/2}$ spectrum might be readily explicable in terms of the Iroshnikov-Kraichnan [16] phenomenology. It does of course ignore local anisotropy, but more importantly, it predicts that the fourth order structure function, $S_4(\ell)$, scales linearly in the inertial range; see [17]. Instead, our data are consistent with linear scaling of the third order structure function, $S_3(\ell)$; see Fig. 4, where we show longitudinal and transversal structure functions. The fourth moment structure function exponent is clearly above unity; see Fig. 5.

The structure functions have been calculated from the Elsasser variables $\mathbf{z}^\pm = \mathbf{u} \pm \mathbf{B}/\sqrt{\mu_0 \rho}$. The scalings of \mathbf{z}^+ and \mathbf{z}^- turn out to be similar, so we take the average value. For hydrodynamic turbulence, linear scaling of $S_3(\ell)$ is an exact result [18], but it is also expected for hydromagnetic turbulence [15].

Finally, we consider the structure function exponents, ζ_p , in the scaling relation $S_p(\ell) \propto \ell^{\zeta_p}$ as a function of p , where ℓ is in the inertial range. Here we make use of the extended self-similarity hypothesis [19] and plot $S_p(\ell)$

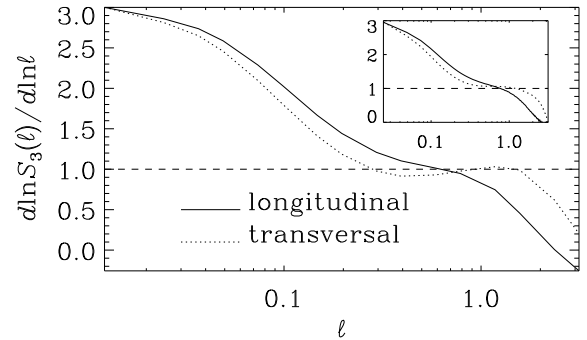


FIG. 4: Third order structure function for runs with 512^3 meshpoints. The inset gives the result for 256^3 meshpoints. The scaling for transversal structure functions (dotted lines) tends to be better than for the longitudinal ones (solid lines). The statistics for the 256^3 runs is somewhat better than for the shorter 512^3 runs.

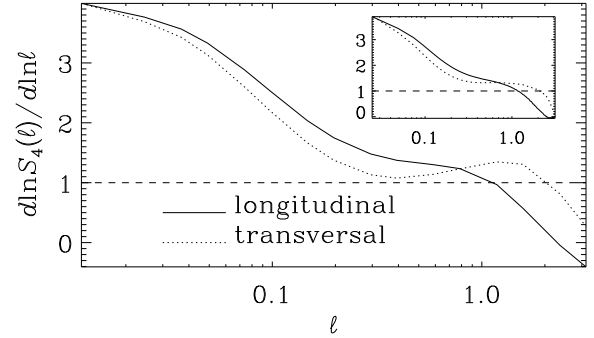


FIG. 5: Same as Fig. 4, but for $S_4(\ell)$. Note that $S_4(\ell)$ is not compatible with linear scaling.

against $S_3(\ell)$ to obtain a more accurate determination of ζ_p . In particular, $\zeta_2 + 1$ is the negative slope of the total energy spectrum: we find $\zeta_2 = 0.70$, which again is consistent with Kolmogorov scaling. For other values of p , the exponents are consistent with the generalized She-Leveque formula [20]

$$\zeta_p = \frac{p}{9} + C \left[1 - \left(1 - \frac{2}{3C} \right)^{p/3} \right], \quad (7)$$

where C is interpreted as the codimension of the dissipative structures. We find that $C = 2$ (corresponding to 1-dimensional, tube-like dissipative structures) gives the best fit to the longitudinal structure function exponents; see Fig. 6. If we allow for fractal codimensions, then $C = 1.85$ gives the best fit for the longitudinal structure function exponents and $C = 1.45$ for the transversal ones. A similar difference has also been reported for incompressible nonmagnetic simulations [21].

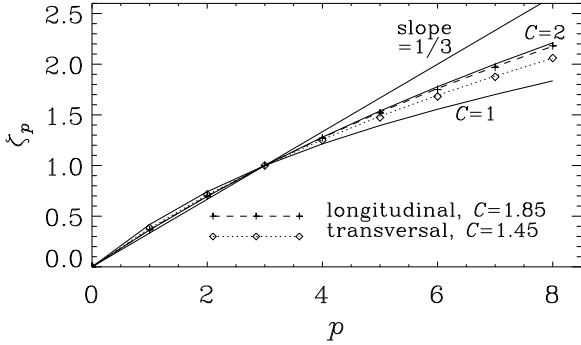


FIG. 6: Exponents ζ_p as a function of p for longitudinal and transversal structure functions. The exponents are between classical She-Leveque scaling ($C = 2$) and Müller-Biskamp scaling ($C = 1$).

Earlier simulations with an external field [22] were consistent with She-Leveque scaling ($C = 2$), while simulations of modestly helical decaying hydromagnetic turbulence [23] suggested that the dominant dissipative structures are current sheets ($C = 1$). Likewise, for highly supersonic turbulence, dissipation occurs mostly in shocks, which are 2-dimensional, so $C = 1$ [24]. This is indeed confirmed by simulations at large Mach numbers [25]. For intermediate Mach numbers the ζ_p are between the scalings for $C = 1$ and 2 [26].

Visualizations of vorticity and current density suggest

that in our simulations the dissipative structures of kinetic energy are mostly tube-like and those of magnetic energy more sheet-like. The fractal codimension found in our simulations is probably explained by a suitable mixture of sheet-like and tube-like dissipative structures.

In summary, we have presented the results of non-helically forced hydromagnetic turbulence simulations at resolutions up to 1024^3 . The scaling of the structure function exponents is consistent with hydrodynamic turbulence where the dissipative structures are believed to be one-dimensional vortex tubes. The energy spectra show what we interpret as a strong bottleneck effect. This effect is particularly strong in the shell-integrated spectra. Throughout the inertial range, however, the magnetic energy exceeds the kinetic energy by a factor of about 2 to 3. Both kinetic and magnetic energies are dominated by the spectral values at the top of the inertial range and independent of magnetic resistivity. The values $\zeta_2 = 0.70$ and $\zeta_3 = 1.0$ strongly favor an asymptotic $k^{-5/3}$ spectrum.

Acknowledgments

We thank Åke Nordlund and Kandaswamy Subramanian for their comments on the paper. Use of the supercomputers in Trondheim (Gridur), Odense (Horseshoe) and Leicester (Ukaff) is acknowledged.

[1] A. Pouquet, U. Frisch, J. Léorat, *J. Fluid Mech.* **77**, 321 (1976).
[2] D. Balsara and A. Pouquet, *Phys. Plasmas* **6**, 89 (1999).
D. Montgomery, W. H. Matthaeus, L. J. Milano, and P. Dmitruk, *Phys. Plasmas* **9**, 1221 (2002).
[3] A. Brandenburg, *Astrophys. J.* **550**, 824 (2001).
[4] J. Maron and E. G. Blackman, *Astrophys. J.* **566**, L41 (2002).
[5] J. Maron and S. C. Cowley, 2001, *astro-ph/0111008*
[6] D. Biskamp and W.-C. Müller, *Phys. Plasmas* **7**, 4889 (2000).
[7] G. Falkovich, *Phys. Fluids* **6**, 1411 (1994).
[8] W. Dobler, N. E. L. Haugen, T. Yousef, and A. Brandenburg, *Phys. Rev. E*, submitted, *astro-ph/0303324* (2003).
[9] We use the Pencil Code which is a grid based high order code (sixth order in space and third order in time) for solving the compressible MHD equations; <http://www.nordita.dk/data/brandenb/pencil-code>.
[10] Z.-S. She and E. Jackson, *Phys. Fluids* **A5**, 1526 (1993). See also G. Falkovich, *Phys. Fluids* **6**, 1411 (1994). D. Lohse and A. Müller-Groeling, *Phys. Rev. Lett.* **74**, 1747 (1995).
[11] K. Subramanian, *Phys. Rev. Lett.* **83**, 2957 (1999).
[12] D. Biskamp, E. Schwarz, and A. Celani, *Phys. Rev. Lett.* **81**, 4855 (1998).
[13] D. H. Porter, P. R. Woodward, and A. Pouquet, *Phys. Fluids* **10**, 237 (1998).
[14] A. Brandenburg, N. E. L. Haugen and W. Dobler, *astro-ph/0303371* (2003).
[15] P. Goldreich and S. Sridhar, *Astrophys. J.* **438**, 763 (1995).
[16] R. S. Iroshnikov, *Sov. Astron.* **7**, 566 (1963). R. H. Kraichnan, *Phys. Fluids* **8**, 1385 (1965).
[17] D. Biskamp *Nonlinear magnetohydrodynamics*. Cambridge University Press (1993).
[18] Frisch, U. *Turbulence. The legacy of A. N. Kolmogorov*. Cambridge University Press (1995).
[19] R. Benzi, S. Ciliberto, R. Tripiccione, C. Baudet, F. Massaioli, and S. Succi, *Phys. Rev. E* **48**, R29 (1993).
[20] Z.-S. She and E. Leveque, *Phys. Rev. Lett.* **72**, 336 (1994).
[21] T. Gotoh, *Comp. Phys. Comm.* **147**, 531 (2002).
[22] J. Cho, A. Lazarian, and E. Vishniac, *Astrophys. J.* **564**, 291 (2002).
[23] W.-C. Müller and D. Biskamp, *Phys. Rev. Lett.* **84**, 475 (2000).
[24] S. Boldyrev, *Astrophys. J.* **569**, 841 (2002).
[25] S. Boldyrev, Å. Nordlund and P. Padoan, *Astrophys. J.* **573**, 678 (2002).
[26] P. Padoan, R. Jimenez, Å. Nordlund, and S. Boldyrev, *astro-ph/0301026* (2003).